Chemistry & Biology, Vol. 12, 371–383, March, 2005, ©2005 Elsevier Ltd All rights reserved. DOI 10.1016/j.chembiol.2005.01.017

Synthetic Erythropoietic Proteins: Tuning Biological Performance by Site-Specific Polymer Attachment

Shiah-Yun Chen,[1] Sonya Cressman,[1,4] Feng Mao,[1,5] Haiyan Shao,[1,6] Donald W. Low,[1] Hal S. Beilan,[1] E. Neil Cagle,[1] Maia Carnevali,[1,7] Vincent Gueriguian,[1] Peter J. Keogh,[1] Heather Porter,[1] Stephen M. Stratton,[1,8] M. Con Wiedeke,[1] Laura Savatski,[2] John W. Adamson,[2] Carlos E. Bozzini,[3] Ada Kung,[1,9] Stephen B.H. Kent,[1,10] James A. Bradburne,[1] and Gerd G. Kochendoerfer[1,*]

[1]Gryphon Therapeutics
600 Gateway Boulevard
South San Francisco, California 94080
[2]The Blood Research Institute
Blood Center of Southeastern Wisconsin
8727 Watertown Plank Road
Milwaukee, Wisconsin 53226
[3]Catedra de Fisiologia
Facultad de Odontologia
Universidad de Buenos Aires
Marcelo T. de Alvear 2142
Buenos Aires 1122
Argentina

Summary

Chemical synthesis in combination with precision polymer modification allows the systematic exploration of the effect of protein properties, such as charge and hydrodynamic radius, on potency using defined, homogeneous conjugates. A series of polymer-modified synthetic erythropoiesis proteins were constructed that had a polypeptide chain similar to the amino acid sequence of human erythropoietin but differed significantly in the number and type of attached polymers. The analogs differed in charge from +5 to –26 at neutral pH and varied in molecular weight from 30 to 54 kDa. All were active in an in vitro cell proliferation assay. However, in vivo potency was found to be strongly dependent on overall charge and size. The trends observed in this study may serve as starting points for the construction of more potent synthetic EPO analogs in the future.

*Correspondence: gkochendoerfer@gryphonrx.com
[4]Present address: Department of Biochemistry and Molecular Biology, Faculty of Medicine, University of British Columbia, 2146 Health Sciences Mall, Vancouver, BC V6T 1Z3, Canada.
[5]Present address: Tanox Corporation, 10301 Stella Link, Houston, Texas 77025.
[6]Present address: Scios Inc., 6500 Paseo Padre Parkway, Fremont, California 94555.
[7]Present address: Department of Chemistry and Biochemistry, University of California, San Diego, Gilman Drive, La Jolla, California 92093.
[8]Present address: Bausch & Lomb, One Bausch & Lomb Place, Rochester, New York 14604.
[9]Present address: Bridge Pharmaceutical, 333 Ravenswood Avenue, Menlo Park, California 94025.
[10]Present address: Departments of Biochemistry and Molecular Biology and Chemistry, The University of Chicago, Chicago, Illinios 60637.

Introduction

Chemical protein synthesis enables the generation of proteins with novel properties [1–4]. The approach is based on the chemoselective ligation of unprotected peptides in aqueous solution. Among the different peptide ligation methods available [5–11], the amide-forming native chemical ligation technique of Dawson et al [6] is the most extensively proven in practical use.

Although the utility of chemical protein synthesis for studying protein structure-function relationships has been considerable, it has only recently been applied to investigate the therapeutic properties of proteins [1, 4, 12, 13]. For example, synthetic analogs of the chemokine CCL5 (RANTES) have been constructed to contain nongenetically encoded modifications in the pharmacophore regions, yielding compounds several orders of magnitude more potent at blocking CCR5-mediated HIV infection than any biologically produced counterpart [13].

We envisioned that beyond changes in the pharmacophore regions, chemical protein synthesis techniques might find use in probing and solving other frequently encountered problems with protein therapeutics, one of which is poor circulating half-life. Our strategy was to produce homogeneous protein conjugates with a constant number of site-specifically attached polymers and to systematically study the effects of varying charge and hydrodynamic radius while keeping the protein backbone and the polymer attachment sites constant. The goal was to determine the dependence of therapeutic properties such as specific activity, circulation lifetime, and immunogenicity on these variables.

Here, we report the design, construction, and biological properties of a series of totally synthetic cytokines designated "synthetic erythropoiesis proteins" (SEPs), which exemplify the utility of this strategy. The peptide backbone of SEP is similar to the sequence of human erythropoietin (EPO), a natural 166 amino acid glycoprotein hormone that regulates the proliferation, differentiation, and maturation of erythroid cells [14].

We previously published a report describing the synthesis and properties of the most potent SEP molecule, SEP-B51 (8–) [12]. In this report, we present the strategy by which this most potent compound was identified, present additional biological characterization of this most potent molecule to date, and discuss how the findings could be applied to produce even more potent SEP analogs.

Results

Design

A total of four different SEP analogs are described in this report. A schematic of the polypeptide backbone and the structures of the polymers attached in the vari-

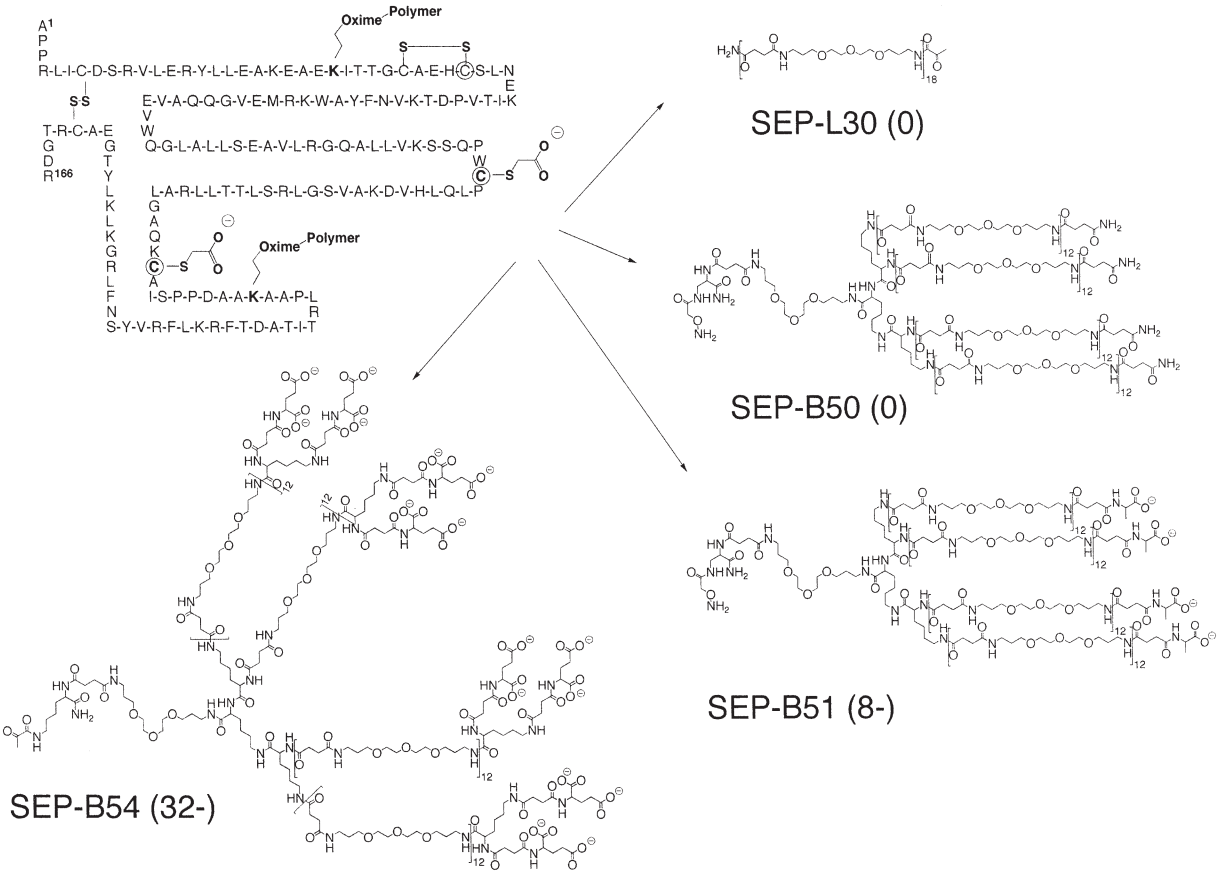

Figure 1. Protein Backbone of SEP and Structure of All Four Different Precision Polymers Employed in This Study

ous SEP analogs is shown in Figure 1. Each of these analogs consisted of an identical polypeptide backbone and two distinct precision polymer entities. The analogs were coded to indicate the protein name (SEP), the nature of the polymer (L for linear, B for branched), and the molecular weight of the construct. Finally, the number in parentheses indicates the total charge imparted on the protein by attachment of two copies of each respective polymer.

The polypeptide backbone of the four SEP analogs was designed to be similar to the backbone of EPO [14] but to possess seven distinct differences in covalent structure. First, the glutamate residues at positions 89 and 117 of EPO were mutated to pseudo-homoglutamate (see below) to facilitate native chemical ligation. Secondly, all native glycosylation sites of EPO were eliminated. Wild-type EPO has three N-linked glycosylation sites in positions Asn^{24}, Asn^{38}, and Asn^{83}, which carry predominantly tetrantennary, branched sugars, as well as an O-linked glycosylation site at position Ser^{126}, contributing an average sugar mass of 12 kDa per EPO monomer. These sites were converted to either lysine residues (amino acid residues Asn^{38} and Asn^{83}) or N^{ϵ}-levulinyl lysine (amino acid residues Asn^{24} and Ser^{126}), respectively. The N^{ϵ}-levulinyl moieties at positions 24 and 126 were incorporated to provide an oxime-forming chemoselective attachment site for a polymer bearing an aminooxyacetyl group in SEP-B50 (0) and SEP-B51 (8–) [7, 15, 16]. For analogs SEP-L30 (0) and SEP-B54 (32–), N^{ϵ}-levulinyl lysine was replaced with N^{ϵ}-aminooxyacetyl lysine in order to attach a pyruvic-acid-bearing polymer [17]. These two sites were chosen among the EPO glycosylation sites for polymer attachment since they are located on opposite faces of the protein, and we speculated that site-specific attachment of a synthetic polymer exclusively to these sites might not interfere with protein function. Finally, the C-terminal amino acid for all SEP constructs was Arg^{166}, which is absent from mature human EPO [18].

The precision polymer moieties were designed to give each SEP molecule a large hydrodynamic radius and an altered clearance profile, as well as a specific net charge at physiological pH. We also speculated that the precision polymers might enhance protein stability by shielding the folded polypeptide from attack by proteolytic enzymes and might reduce immunogenicity of the protein backbone, while retaining full biological potency.

The repeat unit of the precision polymer employed in this study was succinic acid-(4,7,10)-trioxa-1,13-tridecanediamine (see Figure 1). SEP-L30 (0) carried two polymers consisting of 18 repeat units of this polymer with a neutral terminal amide group, resulting in a total molecular weight (peptide backbone plus polymer) of 30 kDa and no additional charges. All other analogs carried a branched polymer that consists of (a) a che-

moselective linker, (b) a hydrophilic spacer consisting of one polymer repeat unit, (c) a core structure having four branching points, (d) a linear polymer having 12 repeat units attached to each branch point, and (e) a charge control unit at the end of each branch. Each branched polymer contributed ~16 kDa to the total molecular weight of each analog. In SEP-B50 (0), each branch carries a neutral amide group, resulting in no additional charges. The SEP-B51 (8–) polymer carried an N^{α}-attached alanyl end group in each branch, resulting in one negative charge per branch or a total of eight negative charges at physiological pH for the two attached polymers. In SEP-B54 (32–), each branch carried a branching core of three N^{α}-attached glutamyl residues, resulting in four negative charges per branch or a total of 32 negative charges at physiological pH for the two attached polymers.

Chemical Protein Synthesis

Unprotected peptide segments were prepared by optimized in situ neutralization stepwise solid-phase peptide synthesis [19], and linear precision polymers were assembled by solid-phase assisted polymer synthesis [20]. The branched precision polymers were assembled by solution coupling of individual linear precision polymers to a branching template as described in Experimental Procedures. The sequence of the chemical ligation, modification, and deprotection steps to construct the full-length proteins for SEP-B50 (0) and SEP-B51 (8–) is summarized in Figure 2. This figure also outlines the protecting group strategy employed in the synthesis. In general, each SEP analog was assembled by ligating four separate peptide segments [peptide segments X modified with precision polymer are denoted SEP-X-(PP)]: SEP-A-(PP), SEP-B, SEP-C, and SEP-D-(PP).

Initially, the precision polymer was linked to the desired peptide segments SEP-A and SEP-D by oxime-forming ligation [7]. For analogs SEP-B50 (0) and analogs SEP-B51 (8–), oxime formation was performed between an aminooxy group on the precision polymer construct and a levulinic acid moiety on the peptides. Using this approach, a significant amount of a peptidic side product with a mass loss –18 relative to the starting peptide was found after HF cleavage. In addition, a significant population of this impure peptide was found after the oximation reaction in the unreacted peptide pool. After isolation, it was determined that the side product is not reactive with any aminooxy compounds and therefore most likely results from an intramolecular reaction of the ketone group with a peptide side-chain functionality. However, this side product was not due to the formation of an intramolecular thiazolidine bond between the ketone group and the N-terminal cysteine residue, since it was present to an even larger extent in segment SEP-A, which is devoid of an N-terminal cysteine residue. In addition, this reaction was not reversible after treatment with 1 M methoxylamine, which rapidly cleaves the thiazolidine ring [21, 22]. In order to overcome this problem, analog SEP-L30 (0) and SEP-B54 (32–) explored an alternative oxime bond formed by a pyruvic acid group on the precision polymer and an aminooxy group on the peptides to generate the peptides SEP-A-(PP) and SEP-D-(PP). We found that the starting peptide segments SEP-A and SEP-D could be produced using optimized in situ neutralization Boc chemistry with a much higher yield (>2×) when modified with an aminooxy group compared to the free ketone group. In addition, use of the aminooxy group on the peptide allowed for the use of pyruvic acid as a ketone-bearing moiety on the polymer. Even though levulinic-acid-based oxime bonds were found to be stable at 4°C in neutral buffers for several weeks, they were found to hydrolyze significantly at lower pH and elevated temperatures. In contrast, the pyruvic acid ketone was >99% stable at 4°C in acetate buffer (pH 4) for 6 months and for at least 2 weeks in the same buffer at 37°C. Interestingly, whereas the formation of the levulinic oxime bond was fully reversible in the presence of 1 M aminooxyacetic acid, as demonstrated in the synthesis of SEP-B54 (32–), pyruvic acid oximes were completely stable in the presence of this strong nucleophile, presumably due to the conjugated nature of the resultant oxime.

After polymer attachment, the four peptide segments were ligated by three sequential native chemical ligations [6]. After each ligation step, the desired product was separated from the reactants by reversed-phase HPLC and characterized by ESI-MS. In the first ligation step, segment SEP-C was ligated to segment SEP-D-(PP). After removal of the Acm protecting group on the N-terminal cysteine on the resulting product SEP-C-D-(PP), SEP-B was ligated to SEP-C-D-(PP). Following the first two ligation steps, the cysteine residues at positions 89 and 117 were alkylated with bromoacetic acid to form noncoded amino acid residues with carboxylate side chains (named pseudo-homoglutamate). The objective of this reaction was to block free thiol groups that may interfere with the folding and stability of the full-length protein, without affecting its function. Cys 161 was protected with a picolinyl group [23], and Cys33 was protected by an Acm group, and thus both residues were not modified during this transformation. After deprotection of Cys 161 and removal of the Acm group on the N-terminal cysteine, SEP-A(PP) was ligated to SEP-B-C-D-(PP) to form the full-length protein construct SEP-A-(PP)-B-C-D-(PP). Recovered yields ranged from 40%–70% for each individual ligation step, while deprotection and modification reactions gave recovered individual step yields ranging from 75%–90%. This provided for efficient assembly of sufficient material (300 μg to more than 25 mg based on protein backbone concentration) for subsequent biophysical and biological characterization of each SEP construct.

We also tested an alternative strategy in which a short linear chain consisting of two precision polymer repeat units was first attached to segments SEP-A and SEP-D for the synthesis of SEP-B54 (32–). The objective of this strategy was the generation of a large batch of linear polypeptide with the short precision polymer chain attached. Removal of the precision polymer and subsequent modification would then allow attachment of multiple different polymers to the polypeptide, allowing for the generation of polymer diversity in fewer synthetic steps (see Figure S2 in the Supplemental Data available with this article online). The short precision polymer chains could be removed efficiently (>90%) in

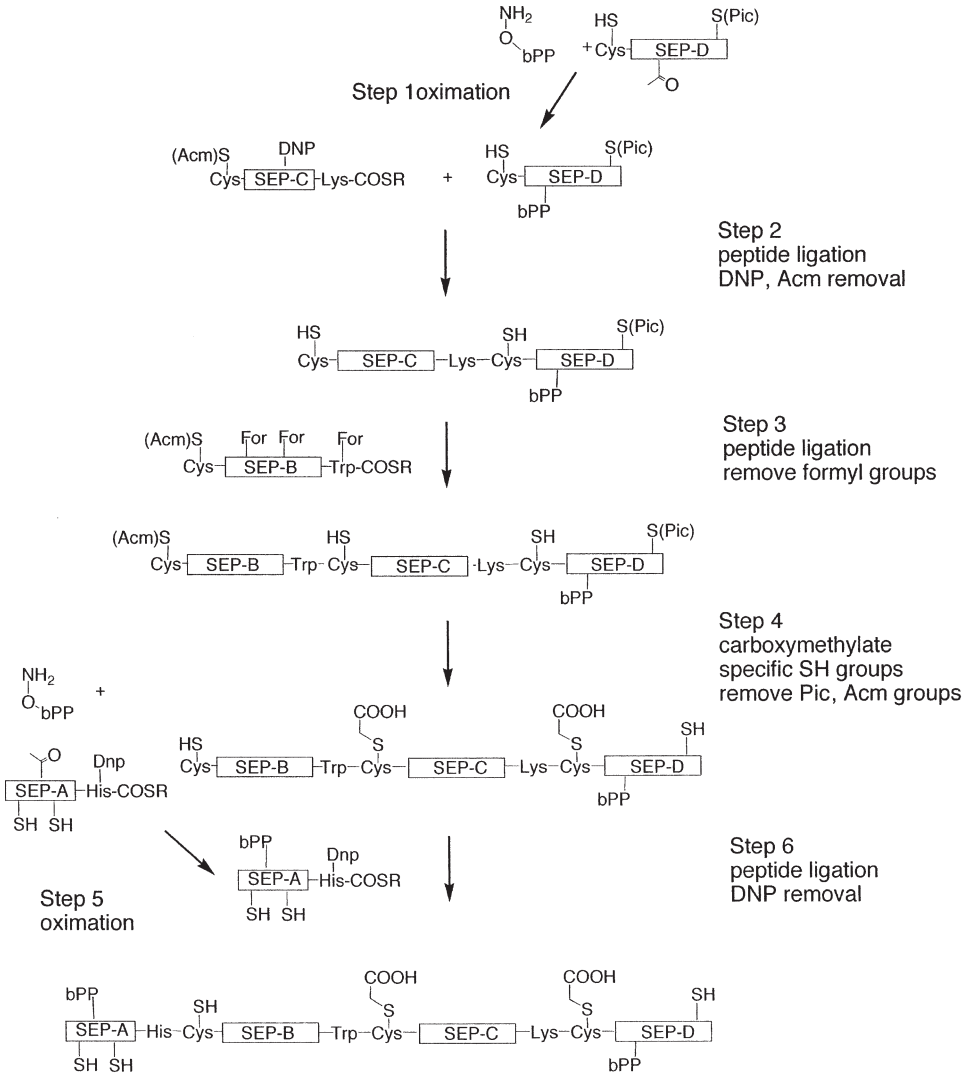

Figure 2. Assembly of SEP Molecules SEP-B51 (8–) and SEP-B50 (0)
Assembly for SEP-B54 (32–) is shown in Figure S2. See main text for details.

50% aqueous acetonitrile containing 0.1% TFA in the presence of 1 M aminooxyacetic acid overnight. Attachment of the branched polymer of SEP-B51 (32–) was achieved after a desalting step, but resulted in recovered yields of only 10%–20%, presumably due to the larger size of the full-length polypeptide chain compared to the individual peptide segments and reduced solubility of the longer peptide chain.

Protein Folding

The synthetic SEP polypeptides were folded in the presence of a redox shuffling agent that was added to control the redox potential of the folding solution and to promote disulfide bond formation and shuffling [24]. The most significant side products of the folding reaction were the formation of misfolded dimeric and oligomeric proteins. Depending on the pI of the target protein, oligomeric species and other impurities were removed by cation exchange or anion exchange purification. A final size-exclusion chromatography step was used to remove residual impurities and to provide for final buffer exchange. Overall folding and purification yields typically ranged from 20%–40% total recovered protein (purity >93%) for all analogs.

Analytical Characterization

A series of complementary analytical techniques were used to unequivocally demonstrate that the SEP molecules were monodisperse, pure, had a defined covalent structure, and were correctly folded. All proteins were characterized by reversed-phase HPLC to assess purity, by electrospray ionization mass spectrometry to determine precise mass, by isoelectric focusing to determine the isoelectric point, and by circular dichroism spectroscopy to assess folding. Figure 3 presents the reversed-phase HPLC chromatograms, electrospray ionization mass spectra, and circular dichroism (CD) spectra for each of the four analogs. In the HPLC chro-

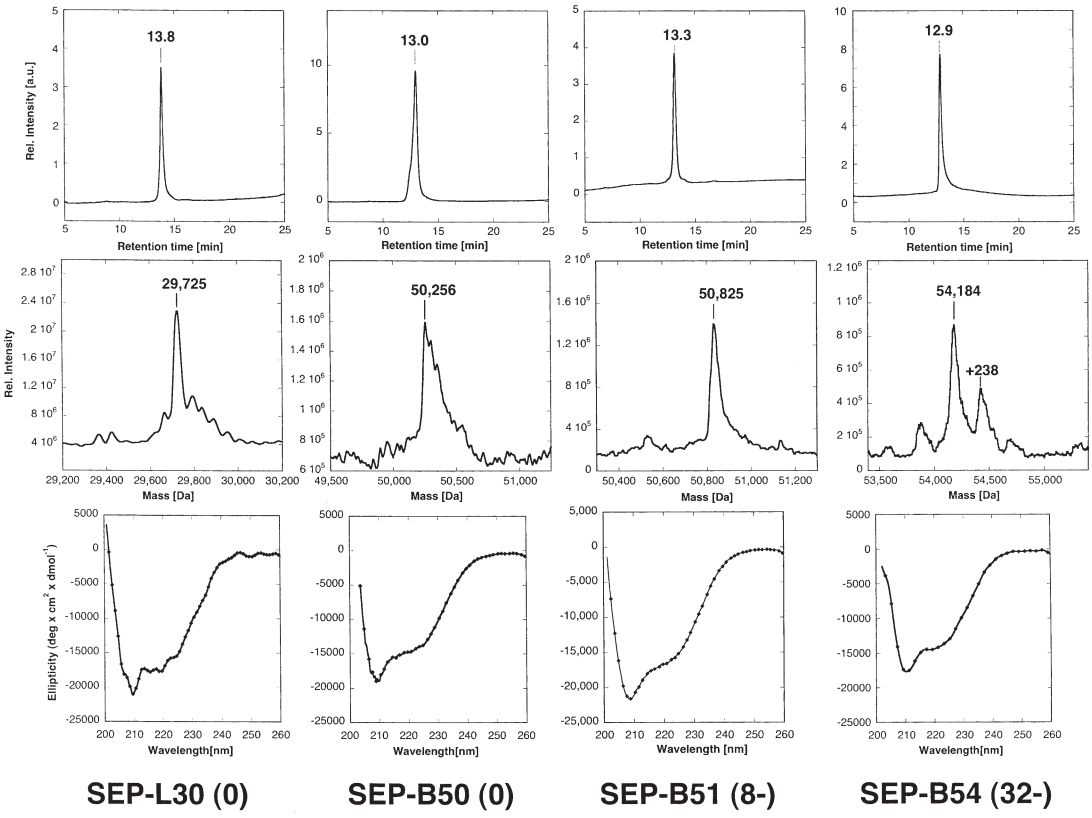

Figure 3. Analytical Characterization of SEP-L30 (0), SEP-B50 (0), SEP-B51 (8–), and SEP-B54 (32–)

Top, reversed-phase HPLC chromatograms of the folded and purified SEP analogs; middle, reconstructed electrospray mass spectra of folded, purified SEP analogs (see also Table 1); bottom row, circular dichroism spectra of all SEP analogs.

matograms, all products exhibited a single peak with a retention time at ~13 min. The shape of the HPLC peaks indicated satisfactory purity, and the small observed shift in retention times between the analogs suggests that the nature of the attached precision polymers does not significantly affect the hydrophobicity of the various SEP analogs. The good correlation of the theoretically calculated mass with the mass observed in the electrospray ionization mass spectra of each analog demonstrated correct assembly of the target structures (see Table 1). A minor satellite band at a mass of –302 Da, which is observed in all products, was assigned to a mixed population of species missing one polymer repeat unit. The ~55 Da mass adduct ladders observed in analog SEP-L30 (0) were most likely due to the chelation of traces of Fe (the isotope distribution is not resolved at such high masses) by the ethylene oxide-containing polymer that is not disrupted by the electrospray ionization process. The same adduct ladders were occasionally observed for the isolated precision polymer. The mass adduct ladders in the spectrum of SEP-B50 (0) were not as well resolved, and therefore assignment is more difficult. The noncovalent nature of the adducts in both cases was confirmed by the dependence of the relative intensity of these peaks on spectrometer orifice potential (data not shown). Finally, analog SEP-B54 (32–) exhibited a significant adduct with a mass of +238. The origin of this adduct could be traced back to the assembly of the branched glutamate cluster at the terminus of the linear precision polymer portions of SEP-B54 (32–), and it thus is only present in one out of eight branches of the polymer in each molecule. We were unable to identify the nature of this adduct. The isoelectric focusing gels exhibited sharp bands for each analog (data not shown). The experimentally determined isoelectric points tabulated in Table 1 were in accord with the predicted isoelectric points based on the molecular composition. To verify that the folding and purification procedures and the attachment of the respective polymers, respectively, did not affect secondary structure formation, CD spectra were acquired in the far UV region between 200 and 260 nm. Figure 3 shows the CD spectra of each of the four SEP analogs. The CD spectra exhibit a negative extremum at 209 nm and a shoulder at around 222 nm, consistent with protein containing predominantly helical and disordered loop structures. The CD spectra of the SEP analogs were thus consistent with the helical structure of a folded long-chain cytokine, indicating that secondary structure formation was independent of the nature of the attached polymer [25].

SEP-B51 (8–) was further characterized by tryptic mapping to confirm site-specific polymer attachment and correct disulfide bond formation. Table S1 lists the

Table 1. Summary of Physical and Biological Properties of the SEP Constructs

	EPO (Multiple Glycoforms)	SEP-L30 (0)	SEP-B50 (0)	SEP-B51 (8–)	SEP-B54 (32–)
Molecular weight (Da) (theoretical)	~30 kDa	29,725 ± 15 (29,706)	50,256 ± 15 (50,253)	50,825 ± 15 (50,821)	54,184 ± 15 (54,167)
Polymer structure	branched sugars	linear PP	branched PP	branched PP	branched PP
Charge on polymer	~–7 to –14	0	0	–8	–32
Total charge at pH = 7	~–2 to –10	+5	+5	–2	–26
PI (IEF)	4.4–5.0	7.9	7.9	5.0	<4
Cell proliferation activity: ED_{50} average of multiple experiments	1.5 ng/ml ± 0.7	5 ng/ml ± 2.1	10 ng/ml ± 3	1.5 ng/ml ± 0.7	5 ng/ml ± 2.1
Posthypoxic mouse model activity (95% confidence interval)	150 mU/ng (standard assigned activity)	no activity at tested concentratios	32 mU/ng (24–41 mU/ng)	150 mU/ng (115–193 mU/ng)	no activity at tested concentrations
Mean residence time (MRT)	5.9 hr ± 1.2	not detectable at t = 5 min[a]	ND	13.0 hr ± 0.8	not detectable at t = 5 min

[a] The PK for SEP-L30 was performed with a structurally comparable analog with a net charge of +3.

peptide fragments expected after tryptic digest of SEP-B51 (8–) arranged by sequence position. Figure S1 presents an RP-HPLC peptide map of the tryptic digest. A total of 17 peaks were designated, and the peaks were labeled from A to R. The peaks were identified by ESI-MS and thus correlated to the expected peptide fragments as presented in Table S1. Every expected peptide fragment was detected with the exception of two dipeptides (amino acid residues 151, 152, and 153, 154) and two individual amino acids (amino acid residues 53 and 140), accounting for >96% (160 out of 166) of the total protein backbone. Peptide fragments P (amino acid residues 21–38) and Q (amino acid residues 117–131) were the only peptide fragments with a mass detected at >16 kDa by ESI-MS. These two fragments contained SEP amino acid residues 24 and 126, respectively (as verified by N-terminal sequencing and ESI-MS), thus confirming site-specific attachment of the branched precision polymer. Peptide fragments I (amino acid residues 5–10 disulfide bonded with amino acid residues 155–162) and P (amino acid residues 21–38) were expected to contain the postulated disulfide bonds. Both fragments were isolated from the HPLC run, lyophilized, and reduced after dissolving into 100 mM phosphate (pH 8.0) and reduction with 100 mM DTT (dithioerythrol) for 1–2 hr at room temperature. After reduction, the peptide fragments were reinjected onto the HPLC column. HPLC-MS analysis of these reduced samples positively identified the expected reduced peptide fragments. These results positively demonstrate the presence of a disulfide bond in SEP-B51 (8–) between the thiol groups on Cys 7 and Cys 161 as well as Cys 29 and Cys 33, respectively.

Cell Proliferation Activity

All SEP analogs were tested for in vitro cell-proliferation activity employing the UT/7 Epo cell line that responds to EPO but not to other related growth factors [26]. Figure 4 shows a representative set of the cell proliferation activity data for SEP-L30 (0), SEP-B50 (0), SEP-B51 (8–), SEP-B54 (32–), and EPO as a function of concentration. All compounds were found to have cell-proliferation acitivity at the concentrations tested as summarized in Table 1 (which presents the averages of multiple experiments for each compound), although the different shapes of the response curves prohibited accurate determination of ED50 values. The presence of cell-proliferative activity confirmed correct folding of all analogs, since misfolded proteins are not expected to have significant biological activity. Several trends were observed. SEP-B51 (8–) had activity comparable to that of EPO. In contrast, the cell-proliferation activity of SEP-L30 (0) and SEP-B54 (32–) was reduced by a factor of ~3, while the cell-proliferation activity of SEP-B50 (0) was reduced by a factor of ~7 relative to EPO (see Table 1). Thus, proteins with significantly greater

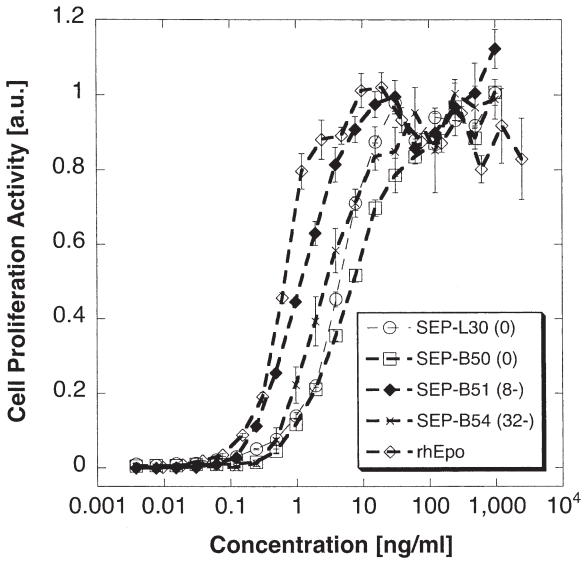

Figure 4. Growth of UT/7 Epo Cells in the Presence of SEP-L30 (0), SEP-B50 (0), SEP-B51 (8–), SEP-B54 (32–), and EPO at Various Concentrations

One representative data set of multiple experiments is shown. Cells were grown in multiwell plates at a concentration of 5000 cells/50 μl. The plates were incubated at 37°C in the presence of 5% CO_2. Cell proliferation was assessed by MTT assay after 5 days. Results shown are the mean of triplicates of one representative experiment.

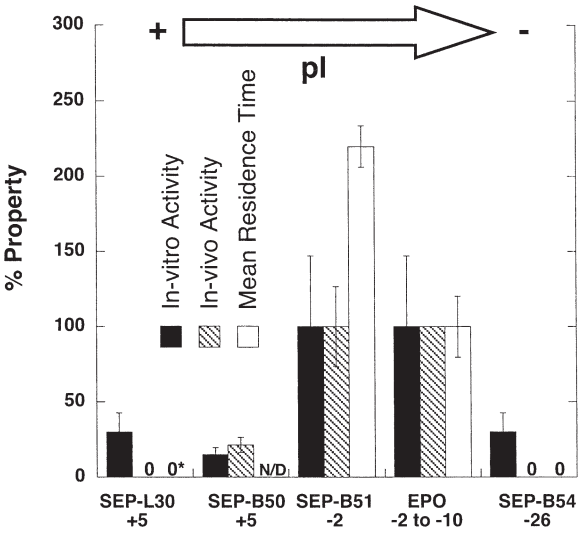

Figure 5. Comparative In Vitro Activity, In Vivo Activity (Posthypoxic Polycythemic Mouse Model), and Mean Residence Time of SEP Analogs Relative to EPO

The proteins are arranged by decreasing experimental isoelectric point, and the net charges of each protein at pH 7 is indicated on the x axis (see main text and Table 1 for experimental methods and results). The PK for SEP-L30 was performed with a structurally comparable analog with a net charge of +3. [The analog of SEP-L30 (0) tested in the PK study had an identical protein backbone and two singly negative linear precision polymers of the same mass attached to identical sites. This analog had very similar in vitro activity to SEP-L30 (0) but did not show any efficacy in normal rats after repeat dosing.]

positive charge [SEP-B50 (0)] or with significantly greater negative charge [SEP-B54 (32–)] had a substantially lower cell-proliferation activity compared to EPO.

In Vivo Activity in the Posthypoxic Polycythemic Mouse Model

Erythropoietic activity of the SEP analogs was evaluated in comparison to EPO in the posthypoxic polycythemia assay in mice [27]. Polycythemia was induced in normal mice by exposure to intermittent hypobaric hypoxia in a simulated high-altitude chamber for a 3 week period, which stimulated endogenous EPO synthesis and secretion and thus increased red cell production. The polycythemic mice were then returned to sea level conditions, which resulted in an almost complete suppression of red cell production. Injection of exogenous erythropoiesis agents into these posthypoxic polycythemic mice transiently stimulated erythropoiesis. The biological response of the polycythemic mice to the erythropoiesis agent was quantified by the percentage of injected Fe^{59} that was incorporated into hemoglobin molecules synthesized in red-cell precursors. Measurement of ^{59}Fe incorporation was performed at a single time point 5 days after the injections of the compounds were determined.

Table 1 and Figure 5 summarize the results from the posthypoxic polycythemic mouse model. SEP-B51 (8–) and EPO had similar activity in this assay. In contrast, SEP-B50 (0) had an activity that was decreased by a factor of five. SEP-B54 (32–) and SEP-L30 (0) did not have any detectable hematopoietic response at comparable doses. These results demonstrate that both the total mass of the polymer and the overall charge of the polymer had a significant impact on the in vivo potency of SEP.

Pharmacokinetics in Rats

Pharmacokinetic studies were consistent with the in vivo activity studies of the respective analogs. SEP-B54 (32–), SEP-B51 (8–), SEP-B50 (0), and a structural analog of SEP-L30 (0) were dosed intravenously in groups of three rats at 5 μg/kg, and the presence of protein-polymer conjugate at different time points was determined by an ELISA assay.

Surprisingly, no protein could be detected even at the earliest time point (t = 5 min) for SEP-B54 (32–), even though the presence of the protein in the dosing solution and compatibility of the syringe and tubing with the protein formulation were verified. This result explains the lack of in vivo activity observed for this analog, as the molecule does not survive sufficiently long in the circulation to exert a significant hematopoietic effect, possibly due to the action of a scavenger receptor.

The pharmacokinetic analysis for the most potent analog, SEP-B51 (8–) has already been reported [12]. The change in plasma concentration of SEP-B51 (8–) with time in male rats receiving a single intravenous dose of 5 μg/kg could be described by a monoexponential pharmacokinetic disposition function with a half-life of 9.5 ± 0.7 hr. The clearance was 3.4 ml ± 0.1 /hr/kg, with mean residence time (MRT) of 13.0 ± 0.8 hr. By comparison, the clearance of EPO was about 7-fold greater than that of SEP-B51 (8–), and the mean residence time of EPO was about 3-fold shorter than that of SEP-B51 (8–).

SEP-B50 (0) was also included in this study, but due to unfortunate circumstances, no data were obtained. However, indirect evidence suggests that SEP-B50 (0) may have comparable lifetimes to SEP-B51 (8–). PK measurements were performed with an analog of comparable backbone that carried two neutral mPEG (polyethylene glycol) molecules in the same positions as in SEP-B50, and lifetimes comparable but slightly shorter than SEP-B51 (8–) were observed. This makes it likely that the lifetime of SEP-B50 is comparable to SEP-B51.

The absence of any in vivo activity for SEP-L30 (0) suggested that this analog is also rapidly cleared. Indeed, a close analog of SEP-L30 (0) [the analog of SEP-L30 (0) tested in the PK study had an identical protein backbone and two singly negative linear precision polymers of the same mass attached to identical sites; this analog had very similar in vitro activity to SEP-L30 (0), but did not show any efficacy in normal rats after repeat dosing] could not be detected at the earliest time point of 5 min after injection at both 5 and 25 μg/kg, consistent with the lack of activity for SEP-L30 (0).

SEP-B51 (8–) Pharmacokinetics and Efficacy in Cynomolgus Monkeys

To get a more detailed understanding of the biological properties of the compound most potent in mice, SEP-

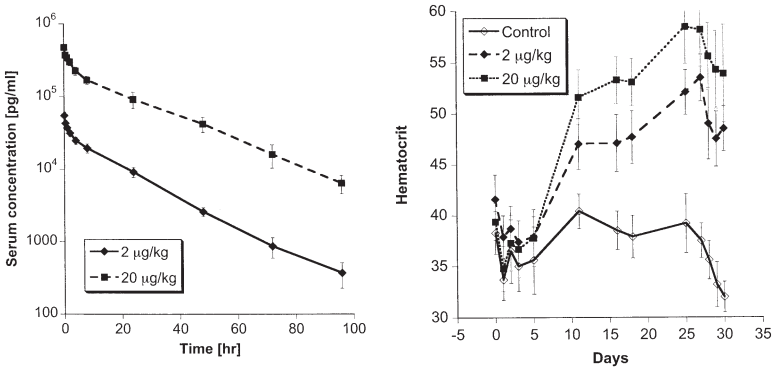

Figure 6. Pharmacokinetics and In Vivo Hematopoietic Activity of SEP-B51 (8–) in Cynomolgus Monkeys at Dose Levels of 0, 2, and 20 μg/kg

At left, groups of six animals were dosed intravenously on day 1. Blood samples were collected for evaluation of the drug concentration over time by ELISA. On the right, subsequently animals were dosed three times a week with the protein concentrations indicated. Blood samples were collected for evaluation of the effect on hematocrit at the indicated time points.

B51 (8–), in a more clinically relevant animal model, a detailed PK and efficacy study in cynomolgus monkeys was performed (Figure 6). In particular, if receptor-mediated mechanisms were important in the clearance mechanism of SEP, as postulated for EPO and other cytokines [28, 29], a significant dose dependence of the SEP clearance would be expected. After single intravenous administration of 2 and 20 μg/kg, SEP-B51 (8–) was cleared from the serum with a slightly shorter mean residence time and elimination half-life following a single dose of 2 μg/kg when compared to 20 μg/kg. As summarized in Table S2, the MRT was determined to be 19 and 25.3 hr for the 2 and 20 μg/kg dose levels, respectively. The elimination half-lives were determined to be 13.7 to 18.5 hr for the 2 and 20 μg/kg dose levels, respectively. The volumes of distribution were comparable for both dose levels within the error of the experiments. The slight dose dependence of the SEP-B51 (8–) clearance suggests that a receptor-mediated clearance mechanism might be contributing to the clearance of SEP-B51 (8–) [28]. In order to see a pharmacological response at these dose levels, additional doses were administered intravenously on day 5 and three times weekly for 3 weeks thereafter. As presented in Figure 6, statistically significant increases in hematocrit were observed on day 11 and showed the expected dose-response relationship. Therefore, SEP-B51 (8–) shows dose-dependent pharmacokinetic properties and stimulates increase in red blood cell volume in a dose-dependent manner in primates.

Discussion

The objective of this study was the systematic exploration of the effect of charge and hydrodynamic radius on the potency of SEP using defined, homogeneous conjugates. Toward this goal, four SEP analogs were prepared and extensively characterized to ensure homogeneity. All constructs had identical polypeptide backbones and polymer attachment sites, but each analog had a distinct net charge and a distinct molecular weight depending on the attached polymers. In this way, the potency and pharmacokinetic properties of the SEP constructs were manipulated by adjusting the polymer structure and charge. As a consequence, the SAR relationships observed could be conclusively assigned to an individual property, such as, e.g., charge, of the molecule.

This is in stark contrast to more traditional studies attempting to correlate hydrodynamic radius and protein charge to potency, such as hyperglycosylation and PEGylation [30–32], which have difficulty establishing unambiguous structure-function relationships. In studies of hyperglycosylated proteins, such as hyperglycosylated recombinant EPO [30], sequence changes are necessary to introduce additional glycosylation sites, and both hydrodynamic radius and overall charge change as a function of the addition of branched, sialylated sugars. Even though in specific cases, notably in reductive alkylation at the N terminus, site-directed PEG attachment with charge conservation is possible, most PEGylation experiments include random attachment of PEG to charged groups, such as lysines [31, 32]. As a result, variation of the number of attached PEG polymers may alter the overall protein charge and modify the attachment site distribution for steric reasons. By contrast, the use of chemical ligation to assemble the polypeptide chain overcomes the issues of sequence and attachment-site variation, whereas the use of precision polymers allows for variation of charge and size without affecting sample homogeneity.

To obtain polymers having a single covalent structure and defined charge, multiple linear and branched polyamide polymers were assembled by a combination of solid-phase organic synthesis [20] and subsequent stoichiometric solution coupling. In particular, branched polymers of up to 16 kDa molecular weight were prepared by condensation of linear blocks of polyamide-polyethyleneoxide polymers onto branching templates [8, 33]. The advantages of stepwise polymer assembly compared to standard solution polymerization [34, 35] include (1) the ability to control the precise length of each polymer segment, (2) the ability to introduce defined branching sites at any desired position, (3) the ability to introduce positive or negative charges at any desired position, and (4) the defined assembly of heteropolymers by direct selection of the monomer unit at each desired position. The homogeneity of our final protein products is a reflection of the high homogeneity of the polymer starting materials employed in these syntheses.

We also had to develop an approach that would permit site-specific attachment of polymers while being

fully compatible with a sequential native chemical ligation and cysteine-masking strategy used for polypeptide assembly. Incorporation of noncoded residues bearing either a side-chain ketone or aminooxy group, respectively, at predetermined positions was accomplished during peptide-chain assembly. The polymers were modified to contain either a single aminooxy or a single ketone group, respectively, that would only react with its complement on the peptide segments to form an oxime bond [7]. Following polymer attachment to two of the four desired peptide segments, assembly of all segments was accomplished by a combination of sequential native chemical ligation, cysteine masking, and folding steps.

Analytical characterization of the folded proteins confirmed their identity, correct folding, their site-specific polymer attachment, and the exceptional homogeneity of the polymers. In particular, tryptic mapping analysis of SEP-B51 (8–) verified the correct covalent structure of the molecules. After protease digestion, chromatographic separation, and ESI-MS analysis, peptide fragments spanning the designed attachment sites, positions 24 and 126, revealed the exclusive presence of polymer in this location. This confirms the utility of oxime formation between the peptide segments and precision polymers to direct the precision polymer to the intended site of attachment.

Biological studies on the SEP analogs established a correlation between several structural features of the attached polymers with potency and circulation lifetime of the resulting proteins. One correlation was the impact of molecular weight on circulating half-life. When tested at similar doses for in vivo hematopoietic activity in the posthypoxic polycythemic mouse model, the SEP construct bearing two large (16 kDa) neutral branched polymers [SEP-B50 (0)] exhibited significant in vivo activity, while the SEP construct with two much smaller (5.5 kDa) neutral linear polymers [SEP-L30 (0)] exhibited no detectable hematopoietic activity. This difference was probably not because of differences in receptor interaction, as SEP-B50 (0) showed comparable in vitro cell proliferation activity relative to SEP-L30 (0) within the error of the measurement. These observations suggest that overall protein size does not significantly affect receptor activation but that there is a size threshold for in vivo activity that lies above the size of SEP-L30 (0) but below the size of SEP-B50 (0).

This threshold is most likely controlled by the renal clearance rate, which in turn depends on the hydrodynamic radius of SEP, as has been demonstrated for other proteins [36]. The hydrodynamic radius of glycosylated EPO is close to the threshold for renal clearance and has been reported as 32 Å (corresponding to a 65 kDa protein such as bovine serum albumin) [25, 37]. Whereas SEP-B51 (8–) eluted earlier by size-exclusion chromatography than BSA, SEP-L30 (0) eluted considerably later. This is consistent with the hypothesis that SEP-L30 (0) is smaller than EPO and thus below the kidney threshold, and that SEP-B51 (8–) is larger than EPO and above the kidney threshold and is thus removed by alternative mechanisms such as receptor-mediated clearance.

Another correlation tested was the impact of the charge of the attached polymers on overall specific activity of the SEP constructs both in vitro and in vivo. Although SEP-B50 (0) exhibited significant activity in the in vitro cell proliferation and in vivo hypoxic polycythemic mouse model assays, these activities were approximately 7-fold and 5-fold less, respectively, than that of SEP-B51 (8–). The reduced activity of SEP-B50 (0) was thus overcome by addition of four negative charges to both polymers in SEP-B51 (8–). This analog showed activity in the in vitro cell proliferation and hematopoietic activity in the posthypoxic polycythemic mouse model that was comparable to EPO. In addition to specific activity, SEP-B51 (8–) displayed superior pharmacokinetic properties and duration of action, as reflected by a 3-fold larger mean residence time, a 7-fold lower clearance, and a substantially higher increase in hematocrit in a normal rat model using both TIW and QW dosing for 4 weeks, as previously reported [12]. Addition of even more negative charge to the polymers in SEP-B54 (32–) led to a marked loss of in vitro cell proliferation activity relative to SEP-B51 (8–). SEP-B54 (32–) also failed to show any hematopoietic activity in the posthypoxic polycythemic mouse model. Consistent with these findings, a pharmacokinetic study for SEP-B54 (32–) found no detectable material in circulation after only 1 hr. Collectively, these results indicate that in vivo activity for the SEP analogs decreases after an apparent maximum in total protein charge and that the net effect of retained specific activity and longer circulation lifetime results in a significantly higher potency for SEP-B51 (8–) compared to EPO.

The most potent compound of this series, SEP-B51 (8–), was further assessed for potency and pharmacokinetic properties in the more clinically relevant cynomolgus monkey model. SEP-B51 (8–) showed an extended lifetime compared to literature values reported for EPO [38] and exhibited dose-dependent clearance and elimination half-lives, suggesting that receptor-mediated clearance may play a significant role. Furthermore, after repeated dosing, a significant dose-dependent pharmacological activity was observed. SEP-B51 (8–) has now been evaluated in a human clinical trial and has shown comparable efficacy in terms of increases in reticulocyte counts comparable with the most potent commercial hyperglycosylated EPO analog [30].

How could we further increase the potency of SEP? Our study suggests that the polymer weight of the larger analogs may be sufficient to avoid renal clearance. There also appears to be a maximum in activity at a polymer charge that is comparable to or larger than 8 but smaller than 32. The most straightforward approach for further optimization would therefore be to systematically explore the charge region between 8 and 32 and to evaluate the effect of charge on overall potency. In addition, the dose dependence of the pharmacokinetic properties suggests involvement of receptor-mediated clearance. A second avenue for further improvement may be to move the polymer-attachment sites to various locations in proximity to the receptor binding sites [39], with the goal of differentially increasing the receptor off-rate and thereby reducing the extent of receptor-mediated endocytosis [40].

In conclusion, we have demonstrated that total chemical protein synthesis can be combined with the

attachment of performance-enhancing polymers to generate homogeneous conjugates and thus to systematically explore the biological properties of polymer-modified proteins.

Significance

Routine production of protein pharmaceuticals by recombinant means is mostly restricted by the use of the 20 coded amino acids as standard building blocks and the difficulty of posttranslational modification of folded proteins with function-enhancing pharmacophores or polymers. Chemical protein synthesis is not limited by either restriction. It is therefore ideally suited to address the known shortcomings of existing protein therapeutics by providing the ability to systematically and rationally modify the biological properties of a lead protein via chemical modification. This approach for the optimization of protein leads is general and can thus be applied to develop new and improve existing protein pharmaceuticals.

Experimental Procedures

Peptide Synthesis

The peptide segments for SEP-B51 (8–) and SEP-B50 (0) were as follows: segment SEP-A (1–32), APPRL ICDSR VLERY LLEAK EAEK(*N*$^{\epsilon}$-levulinyl) I TTGCA EH(Dnp)- thioester; segment SEP-B (33–88), C(Acm)SLNE KIT V PDTKV NFYAW(formyl) KRMEV GQQAV EVW(formyl)QG LALLS EAVLR GQALL VKSSQ PW(formyl)-thioester; segment SEP-C (89–116), C(Acm)PLQL H(Dnp)VDKA VSGLR SLTTL LRALG AQK-thioester; segment SEP-D (117–166), CAISP PDAAK(*N*$^{\epsilon}$-levulinyl) AAPLR TITAD TFRKL FRVYS NFLRG KLKLY TGEAC(picolyl) RTGDR-carboxylate.

The peptides were synthesized on either a thioester-generating resin or a –O-CH_2-Pam (phenylacetamidomethyl) resin by the in situ neutralization protocol for Boc (*tert*butoxycarbonyl) chemistry stepwise solid-phase peptide synthesis [19]. The peptides were deprotected and simultaneously cleaved from the resin support using HF/p-cresol according to standard Boc-chemistry procedures. The resulting peptides were used in unprotected form, with the exception of Cys161(Pic), Cys33(Acm), and Cys89 (Acm), which were differentially protected for reasons of synthetic strategy, and His(Dnp) and Trp(formyl), which were conveniently deprotected during the subsequent ligation reactions and workup steps. For analogs SEP-L30 (0) and SEP-B54 (32–), the N$^{\epsilon}$-levulinyl group was replaced with an N$^{\epsilon}$-aminooxyacetyl group. Synthetic peptides were purified by reversed-phase HPLC and characterized by ESI-MS (electrospray ionization mass spectrometry). Dnp, dinitrophenyl; Acm, acetamidomethyl; Pic, picolyl group.

Precision Length Polymer Synthesis

The structures of the precision polymers of all four SEP analogs are presented in Figure 1. The linear precision polymer was assembled directly on resin. The branched precision polymers were assembled in solution from a template and a linear precision polymer precursor as described below.

Template Synthesis

The template was assembled by solid-phase organic synthesis. For a typical template synthesis, Fmoc-Dpr(Boc-Aoa)-OH (N-α-Fmoc-N-β-(N-*t*.-Boc-amino-oxyacetyl)-L-diaminopropionic acid) was coupled to deprotected Sieber amide resin (Novabiochem, Switzerland). After removal of the Fmoc group, succinic anhydride was coupled in the presence of 0.5 M HOBT (1-hydroxybenzotriazole) and 10% DIEA (diisopropylethylamine) in DMF (dimethylformamide). The free carboxyl group of the resulting resin-bound succinate was activated with 1 M carbonyldiimidazole in DMF. A solution of 50% (4,7,10)-trioxatridecane-1,13-diamine in 0.5 M HOBT in DMF was reacted with the resin-bound activated acid. Fmoc-Lys(Fmoc)-OH, activated with *N*-hydroxysuccinimide and diisopropylcarbodiimide, was then coupled to the resin. After Fmoc group removal, Fmoc-Lys(Fmoc)-OH (HOBT/HBTU/DIEA activated) was coupled to both the α-amine and ϵ-amine of the first resin-bound lysine. Finally, the Fmoc groups were removed, which left four amino groups for reaction with linear precision polymer. After completion of synthesis, the template was cleaved from the resin with 4% v/v TFA (trifluoroacetic acid) in dichloromethane. The cleavage solution was filtered and the template was dissolved in 50% aqueous acetonitrile containing 0.1% TFA. The template was purified after 25-fold dilution by preparative reversed-phase HPLC using a linear water/acetonitrile gradient and lyophilized.

The pyruvic-acid-containing template was synthesized analogously on a RINK-linker substituted resin, except that Fmoc-Lys(Mtt) was coupled to the resin initially, and the branching lysine residues were added using a Boc-Lys (Boc)-N-hydroxysuccinimide ester precursor. After coupling of the final lysine of the branching core, the Mtt side-chain protecting group was removed by multiple treatments with 2% TFA in DCM. After neutralization with 10% DIEA in DMF, pyruvic acid was coupled to the resin after activation with equimolar amounts of DIC and NHS in DCM for 45 min. The Fmoc groups were then removed, and the template was cleaved and purified as described above.

Linear Precision Polymer Precursor Synthesis

Linear precision polymer was assembled on Sasrin resin as described previously [20]. For terminal modification with pyruvate, pyruvic acid was activated with equimolar amounts of NHS and DIC (1,3-diisopropylcarbodiimide) and coupled to the linear polymer at the diamine stage [17]. For terminal modification with a single negative charge, the polymer assembly was stopped at the succinic acid stage, and the terminal carboxyl group was activated with 1 M carbonyldiimidazole in DMF. A 10-fold excess of H-Alanine (OtBu)-HCl was coupled to the resin in the presence of 0.5 M HOBT and 10% DIEA in DMF. For terminal modification with four negative charges, the polymer assembly was stopped at the diamine stage, and Fmoc-Lys(Fmoc)-OH was activated with NHS and DIC (1,3-di-isopropylcarbodiimide) and coupled to the resin. After removal of the Fmoc groups, succinic anhydride was added to the resin, and the free carboxyl group of the resin-bound succinic acids was activated with 0.5 M CDI in DMF. A 10-fold excess of H-Glu(OtBu)-OtBu was coupled in the presence of HOBT and 10% DIEA. After completion of the synthesis, the linear precision polymer precursor was cleaved from the resin with 4% v/v TFA in dichloromethane. The cleavage solution was filtered, the filtrate was dried by evaporation under vacuum, and the dried polymer was dissolved in 50% aqueous acetonitrile. Subsequently, the linear precision polymer precursor was purified by preparative reversed-phase HPLC using a linear water/acetonitrile gradient.

Branched Polymer Assembly

Linear precision polymer precursor was dissolved in anhydrous dimethylsulfoxide, activated with an equimolar amount of HATU [O-(7-azabenzotriazol-1-yl)-1,1,3,3-tetramethyluronium-hexafluoro phosphate] and DIEA, and immediately mixed with the branched template (containing four free amino groups) dissolved in anhydrous dimethylsulfoxide at room temperature. The protected, branched precision polymer was purified by preparative reversed-phase HPLC on a linear water/acetonitrile gradient. The lyophilized, protected branched precision polymer was dissolved in TFA at room temperature to remove the *tert*-butyl and Boc groups as applicable. After TFA removal by evaporation under vacuum and addition of 20% aqueous acetonitrile, the target precision polymer was purified by preparative reversed-phase HPLC with a water/acetonitrile step gradient and lyophilized.

Chemical Protein Synthesis

Oxime-Forming Ligations

A branched or linear precision polymer and one of the peptide segments SEP-D and SEP-A, respectively, were jointly dissolved at a molar ratio of 1:1.2 to 1.5 in 50% aqueous acetonitrile containing 0.1% TFA at a peptide concentration of 10 mg/ml, and the solution was lyophilized. The polymer-modified polypeptide was separated from unmodified polypeptide and unreacted polymer by prepara-

tive RP-HPLC with a linear water/acetonitrile gradient. Fractions containing the desired product SEP-D-(PP) and SEP-A-(PP), respectively, were identified by ESI-MS and/or analytical RP-HPLC, pooled, and lyophilized.

Ligation 1

Segment SEP-D-(PP) was dissolved in neat trifluoroethanol (TFE) and mixed at a molar ratio of 1:1.2 to 1.5 with Acm-protected SEP-C-α-thioester previously dissolved in 6 M guanidine hydrochloride (GnHCl), 300 mM phosphate (pH 7.9). The clear solution was adjusted to a final SEP-D-(PP) peptide concentration of 2 mM and to an organic solvent content of 30% TFE. Thiophenol was added to a final concentration of 1% v/v, and the solution was stirred overnight at room temperature. The ligation mixture was then diluted with 1 volume of 2-mercaptoethanol, 1 volume of TFE, and 3 volumes of 6 M GnHCl, 300 mM phosphate (pH 7.9) to remove residual His(Dnp) protecting groups. The product was purified by preparative RP-HPLC using a linear water/acetonitrile gradient. The Acm protecting group of the product SEP-C-D-(PP) was removed by means of a 3-fold molar excess (relative to the total Acm group concentration) of $Hg(acetate)_2$ for 30 min at room temperature, and the reaction was quenched by addition of β-mercaptoethanol. The reaction product was purified by preparative RP-HPLC using a water/acetonitrile step gradient to yield SEP-C-D-(PP).

Ligation 2

Segment SEP-C-D-(PP) was dissolved in trifluoroethanol (TFE) and mixed at a molar ratio of 1:1.3 to 1.5 with Acm-protected segment SEP-B-α-thioester that had been previously dissolved in 6 M GnHCl, 300 mM phosphate (pH 7.9). The clear solution was adjusted to a final SEP-C-D-(PP) peptide concentration of 1 mM and to an organic solvent content of 30% TFE. Thiophenol was added to a final concentration of 1% v/v, and the solution was stirred overnight at room temperature. A solution consisting of 1 volume of 2-mercaptoethanol, 1 volume of TFE, 3 volumes of 6 M GnHCl, 100 mM acetate (pH 7.9), and 1 volume of piperidine was added to the ligation solution to remove residual His(Dnp) and Trp(formyl) protecting groups. The deprotected product was purified by preparative RP-HPLC using a linear water/acetonitrile gradient to yield Acm-protected SEP-B-C-D-(PP).

Carboxymethylation and Deprotection

Acm-protected SEP-B-C-D-(PP) was dissolved in TFE at 1 mM concentration and diluted with 10 volumes of 6 M GnHCl, 300 mM phosphate (pH 7.9). A 25-fold excess of bromoacetic acid (relative to free thiol groups) dissolved in methanol was added, and the solution was allowed to react for 1 hr. The product was purified by preparative RP-HPLC column with a step gradient to give Acm-protected SEP-B-C-D-(PP) carboxymethylated at residues Cys^{89} and Cys^{117}. For picolyl protecting group removal, zinc dust was activated by stirring in 2 M HCl for 30 min. Acm-protected, carboxymethylated SEP-B-C-D-(PP) was dissolved in neat TFE at about 30 mg/ml. The solution was diluted with 4 volumes of 6 M GnHCl, 50 mM glycine (pH 2.2), containing 35 mg/ml L-methionine, 35 mg/ml sodium dodecanoylsarcosine, and 10% TFE. The solution was then added to the activated zinc powder. After completion of the deprotection reaction, the supernatant was removed and the remaining zinc powder was washed three times to remove adsorbed product. Sodium dodecanoylsarcosine detergent was removed from the solution of product by treatment with Biobeads SM 2 adsorbent. The product was purified by preparative RP-HPLC using a step gradient. The Acm protecting group removal was then performed with $Hg(OAc)_2$ as described above to yield carboxymethylated SEP-B-C-D-(PP).

Ligation 3

Carboxymethylated SEP-B-C-D-(PP) was dissolved in a TFE/6 M GnHCl, 300 mM phosphate (pH 7.9) mixture (1:2) and then combined at a molar ratio of 1:1.2 to 1.5 with segment SEP-A-(PP)-α-thioester previously dissolved in 6 M GnHCl, 300 mM phosphate (pH 7.5). The clear solution was adjusted to a final SEP-B-C-D-(PP) peptide concentration of 1 mM and to an organic solvent content of 30% TFE. Thiophenol was added to a final concentration of 1% v/v, and the solution was stirred overnight. The product was purified by preparative RP-HPLC. HPLC fractions were analyzed by mass spectrometry and analytical RP-HPLC, and those containing the unfolded full-length polypeptide product were combined for the following folding steps.

All analog molecules were prepared following a comparable procedure, except for SEP-B54 (32–).

Synthesis of SEP-B54 (32–)

SEP-B54 (32–) was assembled employing a strategy that relied on the protection of the N^{ϵ}-aminooxyacetylgroup with a two-repeat unit precision polymer. After peptide assembly as described above, a small linear precision polymer [two repeat units of Succinic acid-(4,7,10)-trioxa-1,13 tridecanediamine) capped with levulinic acid] was linked to the polymer attachment site using the same conditions as described above for the oximation with larger precision polymers. Subsequently, the full-length peptide chain was assembled as described above to arrive at the full-length peptide chain.

Taking advantage of the lability of the oxime bond to strong nucleophiles at low pH, the short linear precision polymer was displaced in a solution of 1 M aminooxyacetic acid in 6 M guanidinum chloride (pH 2), resulting in the full-length polypeptide chain now carrying two free aminooxy groups. The product was desalted by preparative RP-HPLC in order to remove aminooxyacetic acid using a step gradient. HPLC fractions were analyzed by mass spectrometry and analytical RP-HPLC, and those containing the deprotected full-length polypeptide product were combined for the subsequent oximation step, resulting in a solution of the full-length peptide of ~1 mg/ml in ~50% aqueous acetonitrile containing 0.1% TFA. For oximation, a 10-fold molar excess of the 16-fold negatively charged branched precision polymer of SEP-B54 (32–) was added to this solution. The product was purified by preparative RP-HPLC. HPLC fractions were analyzed by mass spectrometry and analytical RP-HPLC, and those containing the unfolded full-length polypeptide product were combined for the folding steps.

Folding and Purification

The full-length, polymer-modified polypeptide product was folded using a stepwise dialysis method. Initially, the polypeptide was diluted to a protein concentration of 0.1 mg/ml into HPLC buffer (40% isopropanol and 20% acetonitrile in 0.1% aqueous TFA) containing 6 M GnHCl and 100 mM Tris-HCl (pH 8.5). This solution was then dialyzed overnight into the first folding buffer (3M GnHCl, 100 mM Tris-HCl [pH 8.5]) in the presence of a redox couple (8 mM glutathione [reduced], 1 mM glutathione [oxidized]). The buffer was then exchanged to the second folding buffer (1 M GnHCl, 100 mM Tris-HCl [pH 8.0]) by dialysis for 8 hr. Finally, the buffer was exchanged to 10 mM HPO_4^- (counterion sodium) or 10 mM Tris-HCl (pH 7.0), overnight, respectively. The folded protein solution was then concentrated to 2–2.5 mg/ml by stirred-cell or centrifugal ultrafiltration devices. Depending on the net charge of the desired product, purification was achieved on either Q-Sepharose anion exchange chromatography (initial buffer: 10 mM Tris-HCl) or Resource-S cation exchange chromatography (initial buffer: 10 mM HPO_4^- [counterion sodium]) using gradients of 0–500 mM NaCl for elution. If desired, the concentrated protein solution was further purified by size-exclusion chromatography on a Sephacryl S-300 column using 10 mM Tris-HCl (pH 7.5), 100 mM NaCl as the running buffer.

CD Spectroscopy

Purified SEP analogs were diluted to a final concentration of ~50 μg/ml in 1 mM Tris-HCl (pH 7.0), 20 mM NaCl. Protein concentrations were determined using an extinction coefficient of 1.61 OD/(ml/mg) cm. Spectra were acquired with a JASCO-J700 CD spectrometer at 20°C between 200 and 260 nm in 0.4 nm increments (bandwidth, 1 nm; dwell time, 2s; averaged over ten acquisitions).

HPLC Analysis and Tryptic Peptide Mapping Characterization

Analytical reversed-phase HPLC of folded SEP analogs was performed with a linear gradient of 25%–85% buffer B (60% isopropanol, 30% acetonitrile and 10% water containing 0.08% TFA) versus 0.1% aqueous TFA over 24 min on a Vydac C-4 analytical column. Products were detected at 214 nm. The SEP-B51 (8–) sample solution was digested with trypsin protease in a substrate:enzyme ratio of 50:1 (w:w) at 37°C. After digestion, the resulting peptide fragments were separated by RP-HPLC. Analytical reversed-phase HPLC was performed on aliquots with a linear gradient of 0%–45%

buffer C (acetonitrile containing 0.08% TFA) versus 0.1% aqueous TFA over 60 min on a Vydac C-4 analytical column. Peaks were collected and identified by ESI-MS as well as N-terminal sequencing analysis.

Activity Assay in Human UT/7 EPO Cells

In vitro cell proliferation activities of the analogs and of EPO as a reference standard were determined in a factor-dependent cell-line proliferation assay. Stock solutions of the proteins in Iscove's modified Dulbecco's medium, 10% FBS (fetal bovine serum), glutamine, and Penstrep, and serial 2× dilutions of this stock solution were added to multiwell plates to which human UT/7 EPO cells [26] at a concentration of 5000 cells/50 μl were added. The plates were incubated at 37°C in the presence of 5% CO_2 and monitored daily for growth. After 4 days, 20 μl of 2.5 mg/ml methylthiazoletetrazolium in PBS was added, and the plates were incubated for 4 hr. 150 μl isopropanol was added and the absorbance of each well was read at 562 nm. The activity was corrected for background activity and normalized for the final plateau absorbance. Concentrations were given as the concentration of the polypeptide chain.

Posthypoxic Polycythemic Mouse Model

Groups of 10 mice each (vehicle control, EPO at four dose levels, and SEP analogs at four dose levels) were exposed 18 hr per day to atmospheric air maintained at 506.5 mb in a simulated high-altitude chamber for 20 days (days 1–20). Iron dextran (2 mg) was injected before exposure to assure adequate iron stores and permit the development of polycythemia. Four days after the end of this pretreatment (day 24), the vehicle or dilutions of EPO or the SEP analogs were injected intravenously (IV) in a 200 μL volume. Two days later (day 26), each mouse was injected intraperitoneally (i.p.) with 0.2 μCi of ^{59}Fe. Three days after radioiron injection, mice were bled and hematocrit was determined by the microhematocrit method. The amount of ^{59}Fe (cpm-BG) present in 0.5 ml of blood was then measured in a web-type scintillation counter. The 72 hour-RBC^{59}Fe uptake for each animal was calculated and represents the response. Data from mice with hematocrits below 52% at the time of euthanasia were discarded. Data from each animal and from different groups were statistically analyzed through linear regression analysis. The statistical model used was the "parallel-line" model, in which the relationship between the logarithm of the dose and the response can be represented by a straight line over the range of doses used.

Pharmacokinetics in Rats

A single dose of SEP analogs or EPO was administered intravenously to groups of six male rats on day 1. Blood samples were collected predose and at 5, 30, and 60 min and 2, 4, 8, 24, 48, 72, 96, 120, 144, and 168 hr post-dose. The Quantikine ELISA (R&D System) for EPO was used to assay plasma concentration of SEP and EPO according to the manufacturer's instructions. Serum samples were analyzed at three dilutions in duplicate. A least-squares analysis of the logarithms of the concentrations was performed, and the pharmacokinetic parameters were extracted.

PK/PD Study in Cynomolgus Monkeys

Groups of six animals were dosed intravenously on days 1, 5, 7, 9, 11, 13, 16, 18, 20, 23, 25, and 27 with SEP-B51 (8–) at protein backbone concentrations of 0, 2, and 20 μg/kg. After the first injection, samples of blood for ELISA analyses were collected via venipuncture into tubes without anticoagulant at 5, 30, and 60 min and at 2, 4, 8, 24, 48, 72, and 96 hr post dosing. The Quantikine ELISA (R&D System) for EPO was used to assay plasma concentration of SEP and EPO according to the manufacturer's instructions. Serum samples were analyzed at three dilutions in duplicate. A least-squares analysis of the logarithms of the concentrations was performed, and the pharmacokinetic parameters were extracted. For efficacy determination, samples were collected on days 1, 2, 3, 5, 11, 16, 18, 25, 27, 28, 29, and 30, and the hematocrit was determined by measurement of the packed cell volume for each time point immediately after blood collection.

Supplemental Data

Supplemental Data, including two tables and two figures, are available at http://www.chembiol.com/cgi/content/full/12/3/371/DC1.

Acknowledgments

We thank Midwest Biotech for the large-scale custom synthesis of Boc-Cys(Pic)-OH, Sandra J. Phillips for the coordination of the in vivo studies, and Carol E. Green, Yvonne Freund, and Lori Olson (SRI international) for help with the PK/PD studies. We also thank Young Moo Lee of the University of California at Davis Molecular Structure Facility for N-terminal sequencing assistance. At the time this work was carried out, the majority of the authors were employees of Gryphon Therapeutics, a for-profit biopharmaceutical company in South San Francisco.

Received: October 28, 2004
Revised: January 3, 2005
Accepted: January 27, 2005
Published: March 25, 2005

References

1. Wilken, J., and Kent, S.B. (1998). Chemical protein synthesis. Curr. Opin. Biotechnol. *9*, 412–426.
2. Kochendoerfer, G.G., and Kent, S.B.H. (1999). Chemical protein synthesis. Curr. Opin. Chem. Biol. *3*, 665–671.
3. Dawson, P.E., and Kent, S.B.H. (2000). Synthesis of native proteins by chemical ligation. Annu. Rev. Biochem. *69*, 923–962.
4. Kochendoerfer, G.G. (2001). Chemical protein synthesis methods in drug discovery. Curr. Opin. Drug Discov. Devel. *4*, 205–214.
5. Schnölzer, M., and Kent, S.B.H. (1992). Constructing proteins by dovetailing unprotected synthetic peptides: backbone-engineered HIV protease. Science *256*, 221–225.
6. Dawson, P.E., Muir, T.W., Clark-Lewis, I., and Kent, S.B.H. (1994). Synthesis of proteins by native chemical ligation. Science *266*, 776–779.
7. Rose, K. (1994). Facile synthesis of homogeneous artificial proteins. J. Am. Chem. Soc. *116*, 30–33.
8. Shao, J., and Tam, J.P. (1995). Unprotected peptides as building blocks for the synthesis of peptide dendrimers with oxime, hydrazone, and thiazolidone linkages. J. Am. Chem. Soc. *117*, 3893–3899.
9. Saxon, E., Armstrong, J.I., and Bertozzi, C.R. (2000). A "traceless" Staudinger ligation for the chemoselective synthesis of amide bonds. Org. Lett. *2*, 2141–2143.
10. Nilsson, B.L., Kiessling, L.L., and Raines, R.T. (2001). High-yielding Staudinger ligation of a phosphinothioester and azide to form a peptide. Org. Lett. *3*, 9–12.
11. Botti, P., Carrasco, M.R., and Kent, S.B.H. (2001). Native chemical ligation using removable N-α-(1-phenyl-2-mercaptoethyl) auxiliaries. Tetrahedron Lett. *42*, 1831–1833.
12. Kochendoerfer, G.G., Chen, S.Y., Mao, F., Cressman, S., Traviglia, S., Shao, H., Hunter, C.L., Low, D.W., Cagle, E.N., and Carnevali, M. (2003). Design and chemical synthesis of a homogeneous polymer-modified erythropoiesis protein. Science *299*, 884–887.
13. Hartley, O., Gaertner, H., Wilken, J., Thompson, D., Fish, R., Ramos, A., Pastore, C., Dufour, B., Cerini, F., Melotti, A., et al. (2004). Medicinal chemistry applied to a synthetic protein: development of highly potent HIV entry inhibitors. Proc. Natl. Acad. Sci. USA *101*, 16460–16465.
14. Jacobs, K., Shoemaker, C., Rudersdorf, R., Neill, S.D., Kaufman, R.J., Mufson, A., Seehra, J., Jones, S.S., Hewick, R., and Fritsch, E.F. (1985). Isolation and characterization of genomic and cDNA clones of human erythropoietin. Nature *313*, 806–810.

15. Canne, L.E., Ferré-D'Amaré, A.R., Burley, S.K., and Kent, S.B.H. (1995). Total chemical synthesis of a unique transcription factor-related protein: cMyc-Max. J. Am. Chem. Soc. *117*, 2998–3007.
16. Marcaurelle, L.A., and Bertozzi, C.R. (1998). Direct incorporation of unprotected ketone groups into peptides during solid-phase synthesis: application to the one-step synthesis of peptides with two different biophysical probes. Tetrahedron Lett. *39*, 7279–7282.
17. Kochendoerfer, G.G., Tack, J.M., and Cressman, S. (2002). Total chemical synthesis of a 27 kDa TASP protein derived from the MscL ion channel of M. tuberculosis by ketoxime-forming ligation. Bioconjug. Chem. *13*, 474–480.
18. Recny, M.A., Scoble, H.A., and Kim, Y. (1987). Structural characterization of natural human urinary and recombinant DNA-derived erythropoietin. Identification of des-arginine 166 erythropoietin. J. Biol. Chem. *262*, 17156–17163.
19. Schnölzer, M., Alewood, P., Jones, A., Alewood, D., and Kent, S.B.H. (1992). In situ neutralization in Boc-chemistry solid phase peptide synthesis. Int. J. Pept. Protein Res. *40*, 180–193.
20. Rose, K., and Vizzavona, J. (1999). Stepwise solid-phase synthesis of polyamides as linkers. J. Am. Chem. Soc. *121*, 7034–7038.
21. Villain, M., Vizzavona, J., and Rose, K. (2001). Covalent capture: a new tool for the purification of synthetic and recombinant polypeptides. Chem. Biol. *8*, 673–679.
22. Villain, M., Vizzavona, J., and Gaertner, H. (2002). Chemical ligation of multiple peptide fragments using a new protection strategy. In Peptides: The Wave of the Future. Proceedings of the 17th American Peptide Symposium., M. Lebel and R.A. Houghten, eds. (Dordrecht, The Netherlands: Kluwer Academic Publishers), pp. 107–108.
23. Gosden, A., Stevenson, D., and Young, G.T. (1972). Protection of thiol and phenolic hydroxy-groups as their 4-picolyl ethers, cleaved by electrolytic reduction. Chem. Commun. *8*, 1123–1124.
24. Saxena, V.P., and Wetlaufer, D.B. (1970). Formation of three-dimensional structure in proteins. I. Rapid nonenzymic reactivation of reduced lysozyme. Biochemistry *9*, 5015–5023.
25. Davis, J.M., Arakawa, T., Strickland, T.W., and Yphantis, D.A. (1987). Characterization of recombinant human erythropoietin produced in Chinese hamster ovary cells. Biochemistry *26*, 2633–2638.
26. Komatsu, N., Yamamoto, M., Fujita, H., Miwa, A., Hatake, K., Endo, T., Okano, H., Katsube, T., Fukumaki, Y., and Sassa, S. (1993). Establishment and characterization of an erythropoietin-dependent subline, UT-7/Epo, derived from human leukemia cell line, UT-7. Blood *82*, 456–464.
27. Alippi, R.M., Barcelo, A.C., and Bozzini, C.E. (1983). Erythropoietic response to hypoxia in mice with polycythemia induced by hypoxia or transfusion. Exp. Hematol. *11*, 122–128.
28. Kato, M., Kamiyama, H., Okazaki, A., Kumaki, K., Kato, Y., and Sugiyama, Y. (1997). Mechanism for the nonlinear pharmacokinetics of erythropoietin in rats. J. Pharmacol. Exp. Ther. *283*, 520–527.
29. Tanaka, H., and Tokiwa, T. (1990). Pharmacokinetics of recombinant human granulocyte stimulating factor studied in the rat by a sandwich enzyme-linked immunosorbent assay. J. Pharmacol. Exp. Ther. *255*, 724–729.
30. Egrie, J.C., and Browne, J.K. (2001). Development and characterization of novel erythropoiesis stimulating protein (NESP). Br. J. Cancer *84*, 3–10.
31. Harris, J.M., and Chess, R.B. (2003). Effect of pegylation on pharmaceuticals. Nat. Rev. Drug Discov. *2*, 214–221.
32. Bailon, P., Palleroni, A., Schaffer, C.A., Spence, C.L., Fung, W.J., Porter, J.E., Ehrlich, G.K., Pan, W., Xu, Z.X., Modi, M.W., et al. (2001). Rational design of a potent, long-lasting form of interferon: a 40 kDa branched polyethylene glycol-conjugated interferon alpha-2a for the treatment of hepatitis C. Bioconjug. Chem. *12*, 195–202.
33. Posnett, D.N., and Tam, J.P. (1989). Multiple antigenic peptide method for producing antipeptide site-specific antibodies. Methods Enzymol. *178*, 739–746.
34. Hai, T.T., Pereira, D.E., Nelson, D.J., Srnak, A., and Catarello, J. (1999). Polymerization of diaspirin cross-linked hemoglobin (DCLHb) with water-soluble, nonimmunogenic polyamide cross-linking agents. Bioconjug. Chem. *10*, 1013–1020.
35. Hai, T.T., Pereira, D.E., and Nelson, D.J. (1998). Synthesis of water-soluble, nonimmunogenic polyamide cross-linking agents. Bioconjug. Chem. *9*, 645–654.
36. Knauf, M.J., Bell, D.P., Hirtzer, P., Luo, Z.P., Young, J.D., and Katre, N.V. (1988). Relationship of effective molecular size to systemic clearance in rats of recombinant interleukin-2 chemically modified with water-soluble polymers. J. Biol. Chem. *263*, 15064–15070.
37. Zhan, H., Liu, B., Reid, S.W., Aoki, K.H., Li, C., Syed, R.S., Karkaria, C., Koe, G., Sitney, K., Hayenga, K., et al. (1999). Engineering a soluble extracellular erythropoietin receptor (EPObp) in Pichia pastoris to eliminate microheterogeneity, and its complex with erythropoietin. Protein Eng. *12*, 505–513.
38. Ramakrishnan, R., Cheung, W.K., Farrell, F., Joffee, L., and Jusko, W.J. (2003). Pharmacokinetic and pharmacodynamic modeling of recombinant human erythropoietin after intravenous and subcutaneous dose administration in cynomolgus monkeys. J. Pharmacol. Exp. Ther. *306*, 324–331.
39. Syed, R.S., Reid, S.W., Li, C., Cheetham, J.C., Aoki, K.H., Liu, B., Zhan, H., Osslund, T.D., Chirino, A.J., Zhang, J., et al. (1998). Efficiency of signalling through cytokine receptors depends critically on receptor orientation. Nature *395*, 511–516.
40. Darling, R.J., Kuchibhotla, U., Glaesner, W., Micanovic, R., Witcher, D.R., and Beals, J.M. (2002). Glycosylation of erythropoietin affects receptor binding kinetics: role of electrostatic interactions. Biochemistry *41*, 14524–14531.